Fish and Shellfish Immunology 92 (2019) 64–71

Contents lists available at ScienceDirect

Fish and Shellfish Immunology

journal homepage: www.elsevier.com/locate/fsi

Short communication

Immune-related molecular and physiological differences between black-shelled and white-shelled Pacific oysters *Crassostrea gigas*

Lei Wei[a,1], Qiuyun Jiang[a,d,1], Zhongqiang Cai[b], Wenchao Yu[a], Cheng He[a], Wen Guo[c], Xiaotong Wang[a,*]

[a] School of Agriculture, Ludong University, Yantai, 264025, China
[b] Changdao Enhancement and Experiment Station, Chinese Academy of Fishery Sciences, Changdao, 265800, China
[c] Marine Biology Institute of Shandong Province, Qingdao, 266104, China
[d] National Demonstration Center for Experimental Fisheries Science Education, Shanghai Ocean University, Shanghai, 201306, China

ARTICLE INFO

Keywords:
Pacific oysters
Different melanin content
Immune recognition and modulation
Apoptosis and phagocytosis
Oxidative stress

ABSTRACT

The black-and-white traits on shells and mantle edges of the Pacific oyster, *Crassostrea gigas*, are inheritable and correlated, and black shells (melanin pigmentation) are usually found in the Pacific oysters. Based on differentially expressed genes from RNA-Seq and physiological characteristics, in this study, Black-shelled Pacific oysters (BSO) and White-shelled Pacific oysters (WSO) were selected to determine the molecular differences between oysters with obviously different melanin content. The differences in the process of immune recognition and modulation indicated that BSO may be more sensitive to the immune substances. There might have different modulation mode of apoptosis and phagocytosis between BSO and WSO, and caspase-3 might have played a key role in the apoptotic process of BSO. Different oxidation-related pathways were enriched in both BSO and WSO, suggesting the different response strategies of BSO and WSO to oxidative stress. The physiological evidences showed that, compared with WSO, in BSO, the tyrosinase content, the caspase-3 activity and the suppression of hydroxyl radical increased, and the reactive oxygen species concentration decreased. Therefore, immune-related molecular and physiological differences were found between BSO and WSO.

1. Introduction

The Pacific oyster *Crassostrea gigas* is the important aquaculture species around the world. Shell color is one of the important traits in oysters breeding. Previous researches have shown that the two color traits (black and white) on shells and mantle edges of Pacific oysters are inheritable and correlated, enabling effective selection for the color traits [1]. The black pigment in oyster shells, mantles and adductor muscle scars was confirmed to be melanin by ultraviolet and infrared radiation spectral analysis [2]. In Pacific oyster individuals, differences in melanin pigmentation are usually found in the shell and mantle. However, the role of melanin pigmentation in Pacific oysters has not been fully understood.

Melanin exists widely in nature and is a key pigment synthesized in molluscs *in vivo* [3]. Previous studies have shown that a series of cellular biological processes are associated with melanosis in organisms [4]. In vertebrates, the melanin is secreted and transferred into the keratinocytes of the epidermis and hair to protect the skin and eyes against UV radiation [5]. The large amount of melanin deposited on bird feathers can reflect the regulatory capacity of cellular immune response [6]. In invertebrates, melanin formation is the prominent immune responses of insects [7], and the melanization is the major aspect of the innate immune defense system against invading pathogens in which melanin participates, in the meanwhile, the generation of free radical by-products could aid in their killing [8]. Recent studies indicate that fungal melanin is immunologically active, and the protein melanin-sensing C-type lectin receptor (Mellec) recognizes melanin and plays an essential role in protecting antifungal immunity in both mice and humans, which suggested melanin could trigger antifungal defenses [9,10].

The biosynthesis of melanin is caused by the action of tyrosinase (TYR). TYR catalyzes two distinct reactions of melanogenesis, and also plays an important role in the formation of the shell matrix of the pearl oyster *Pinctada fucata* [11,12]. There are at least 26 TYR isoforms in the genome of the Pacific oyster, which can be divided into three basic types: secretory, intracellular and transmembrane type [13,14].

* Corresponding author.
E-mail address: wangxiaotong999@163.com (X. Wang).
[1] These authors contributed equally to this work as first authors.

https://doi.org/10.1016/j.fsi.2019.05.056
Received 16 November 2018; Received in revised form 15 April 2019; Accepted 25 May 2019
Available online 28 May 2019

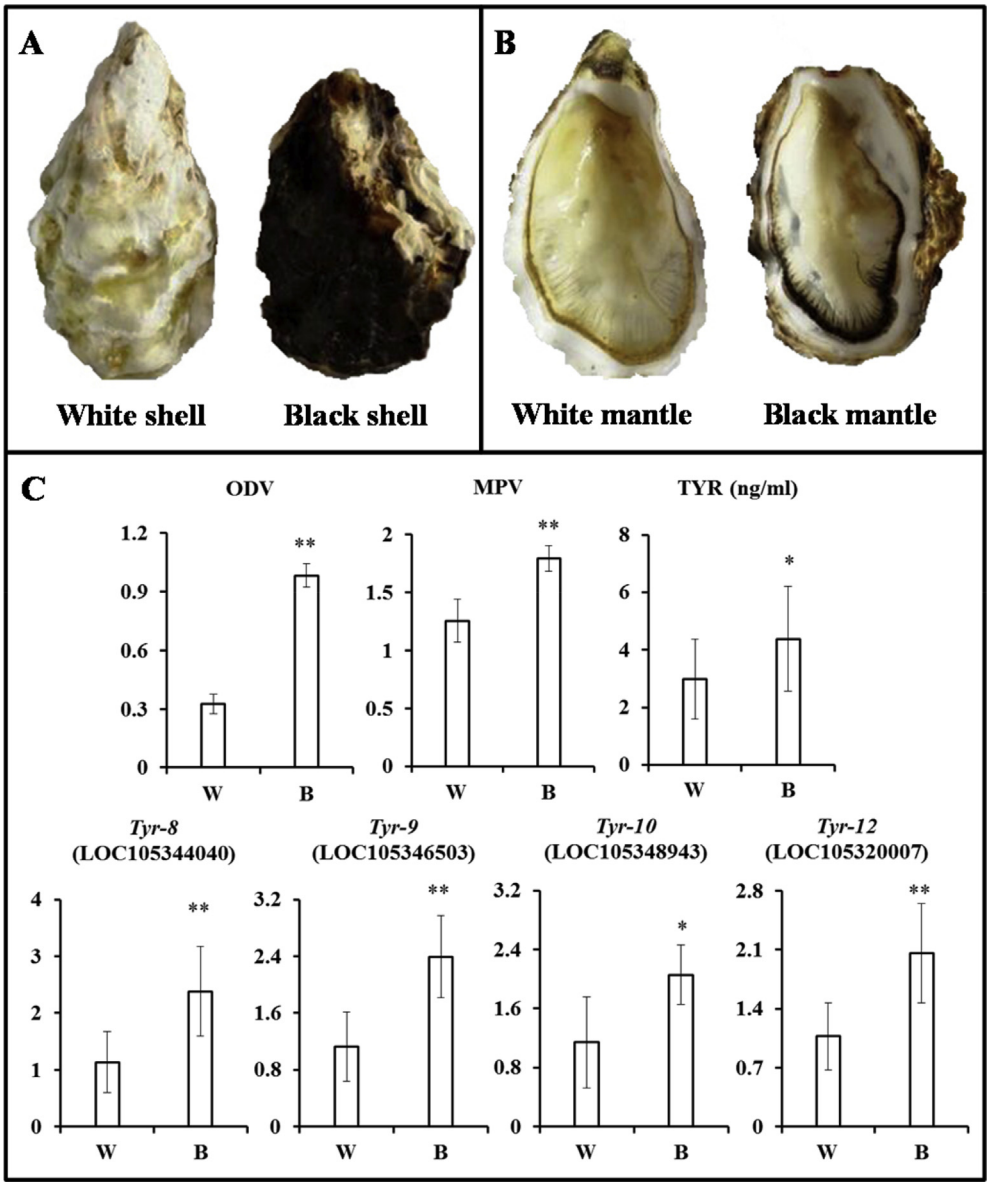

Fig. 1. Pigmentation of Pacific oyster shells and mantle edges. (A) The white and black shells of Pacific oyster. (B) The white and black mantles of Pacific oyster. (C) The optical density values (ODV) of shell pigmentation determined by the grayscale comparison; the mantle edge pigmentation values (MPV) of Pacific oysters; the TYR content; the relative mRNA expression profiles of 4 Tyr. Each bar represents the mean ± S.D. (n = 12). * indicated $P < 0.05$. ** indicated $P < 0.01$. Abbreviations: W, white-shelled Pacific oysters (WSO); B, black-shelled Pacific oysters (BSO).

Preliminary studies have shown that different members of the TYR gene families could play a role in independent pigmentation in different organs of Pacific oysters [15].

In the current study, two groups of Pacific oysters in different shell colours with different melanin contents were established: Black-shelled Pacific oysters (BSO) and White-shelled Pacific oysters (WSO). Then, RNA-Seq was used to provide a comprehensive understanding of molecular mechanisms of these two kinds of Pacific oysters. Moreover, the different immune strategies were screened out by gene-set enrichment analysis and verified by physiology changes.

2. Materials and methods

2.1. Animal collection

Adult BSO and WSO (shell length: 8–10 cm) were sampled and investigated from the same selective breeding population in Changdao, Yantai City, Shandong Province, China. The oysters were acclimated in filtered (1 μm) and aerated seawater (pH 8.1, temperature 18 °C and salinity 29‰) for 2 weeks before the start of the experiment. During the acclimation period, the oysters were fed with *Isochrysis galbana* at a concentration of 5.0×10^5 cells mL^{-1} three times a day. The seawater was renewed every day. Two experimental groups, BSO and WSO, were selected by the comparison of shell pigmentation according to the methods in Section 2.2.

In RNA-Seq analysis, the mantle tissues of 3 individuals were combined to form one sample; 12 individuals from each BSO and WSO group were randomly selected for related physiological measurements. In addition, 6 other individuals from each group were used for quantitative real-time PCR (qRT-PCR) assays. All the mantle tissues were flash frozen in liquid nitrogen and then stored at −80 °C.

2.2. Measurement of shell pigmentation

To describe the pigmentation of Pacific oyster shells, a digital camera was used to get images of oysters illuminated by two light bulbs

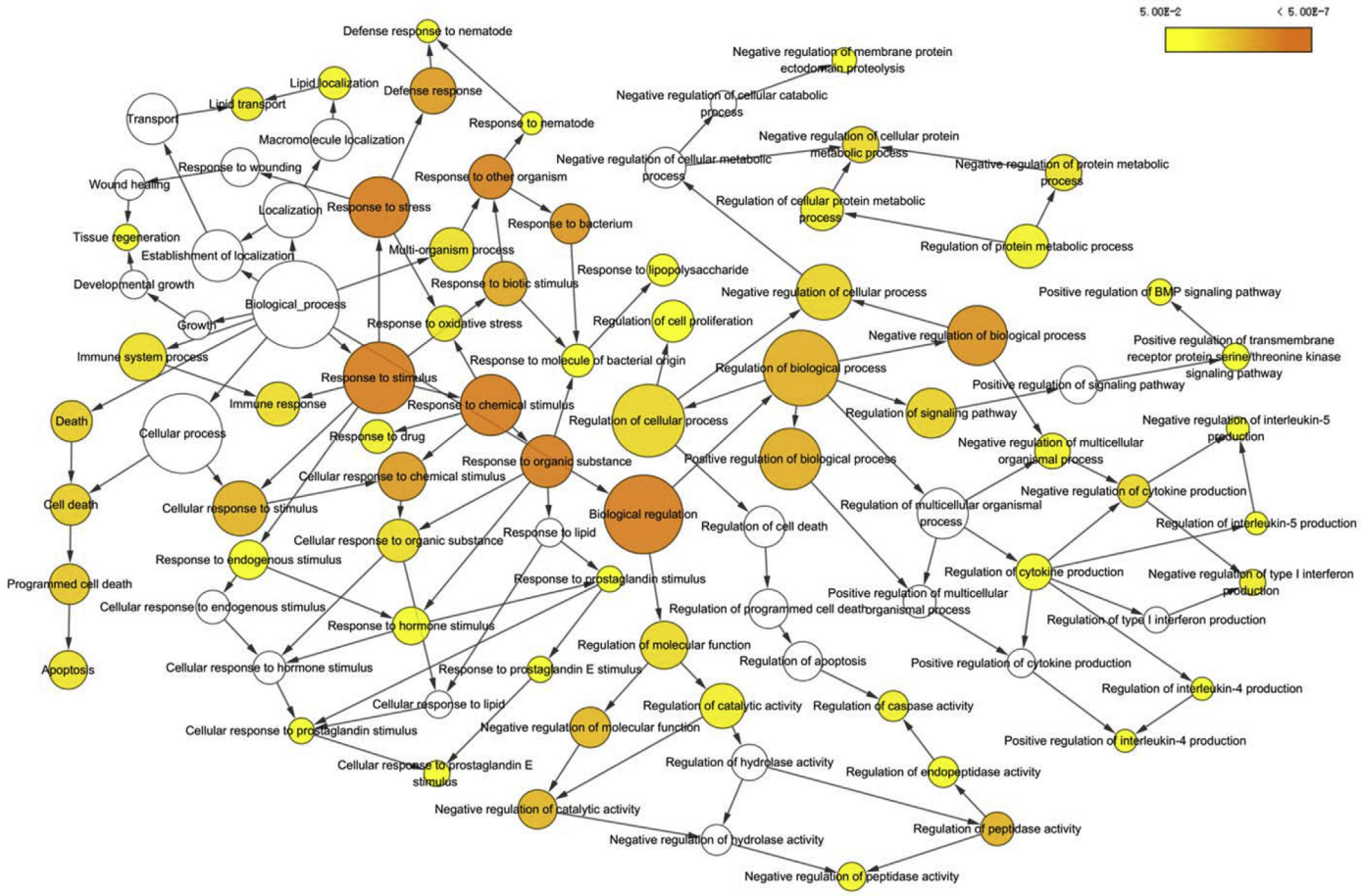

Fig. 2. The BinGO enrichment analysis of up-regulated Gene Ontology biological process (BP) terms in black-shelled Pacific oysters. BP terms are shown as nodes with the node size, and color intensity representing their enrichment and statistical significance. Insignificant BP terms in the network are shown in white. (For interpretation of the references to color in this figure legend, the reader is referred to the Web version of this article.)

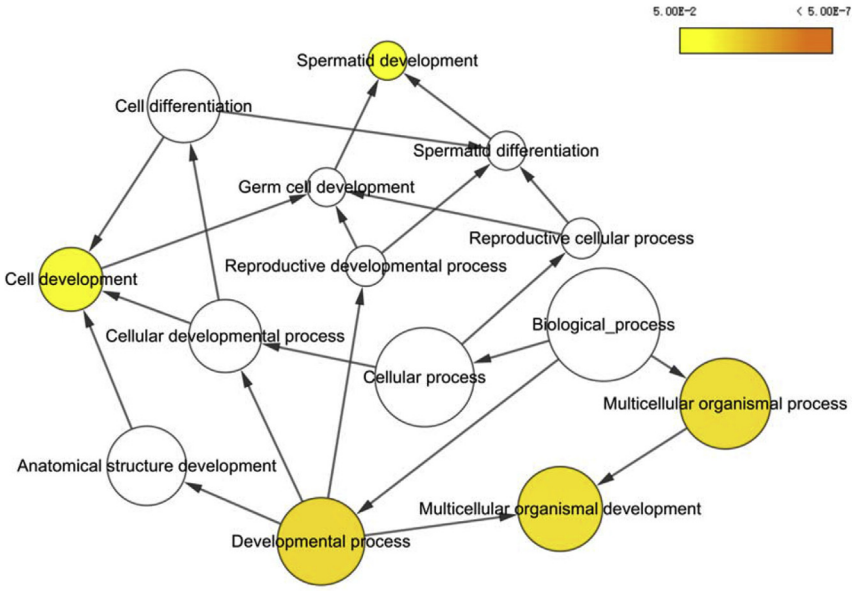

Fig. 3. The BinGO enrichment analysis of up-regulated Gene Ontology biological process (BP) terms in white-shelled Pacific oysters. BP terms are shown as nodes with the node size, and color intensity representing their enrichment and statistical significance. Insignificant BP terms in the network are shown in white. (For interpretation of the references to color in this figure legend, the reader is referred to the Web version of this article.)

mounted on both sides of the sample board. The bulbs provided uniform and consistent illumination for the photography. The optical density of each shell was analyzed by Image-Pro Plus image analysis software 6.0 (Media Cybernetics Inc., USA). The measurement/counting/size/scale regulator was set automatically to the contour of the oyster shells to create areas of interest. The intensity calibration was set to the standard optical density and the gray scale value was converted to an optical density value (ODV), on a scale ranging from 0 (completely white) to 2.4 (completely black). The ODV of each image was measured by using macros as the values of the shell pigmentation.

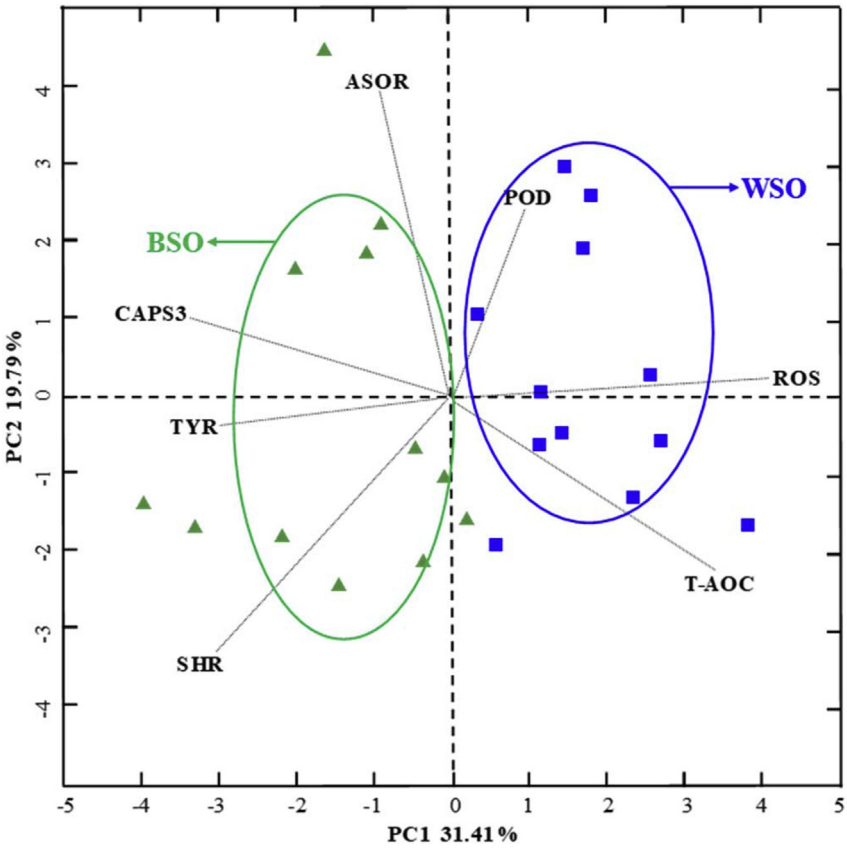

Fig. 4. Biplot containing PC scores of the mantles of black-shelled Pacific oysters (BSO) compared with white-shelled Pacific oysters (WSO). Contributions of BSO (▲) and WSO (■) variables [seven biochemical indices: Tyrosinase content (TYR); suppression of hydroxyl radical (SHR); anti-superoxide anion radical (ASOR); production of reactive oxygen species (ROS); total antioxidant capacity (T-AOC); peroxidase (POD); caspase-3 (CASP3)] to the clustering of oyster samples.

According to ODV [16], the classification were as follows: (1) very light (white, with little or no pigmentation present, ODV 0–0.5); (2) light (having only slight pigmentation, mixed with light hues, ODV 0.5–0.7); (3) dark (showing some dark or black pigmentation, also with light color areas, ODV 0.7–0.9); and (4) very dark (having very dark pigmentation, mostly black, ODV 0.9–1.4). In this study, the oysters confirming to the 'very light' category were used as the WSO samples, while oysters confirming to the 'very dark' category used as the BSO ones.

2.3. RNA preparation and RNA-Seq

Total RNA of Pacific oyster mantles was isolated by TRIzol reagent (Invitrogen, USA), and then subjected to DNAse digestion with RQ1 DNAse (Promega, USA) according to the manufacturer's instructions. RNA integrity was evaluated using Agilent 2100 Bioanalyzer (Agilent Technologies, Santa Clara, CA, USA). Samples with RNA Integrity Number (RIN) ≥ 7 were subsequently analyzed. According to the manufacturer's instructions, these libraries were constructed using TruSeq Stranded mRNA LT Sample Prep Kit (Illumina, San Diego, CA, USA). mRNA was purified, fragmented, and then synthesized to cDNA using SuperScript II Reverse Transcriptase (Invitrogen). The cDNA was purified and adenylated at the 3′ end using A-tailing control (1 μL A-tailing control + 99 μL resuspension buffer). Ligation control (1 μL ligation control + 99 μL resuspension buffer) was then added to ligate adapters on the cDNA. Then the DNA fragment was enriched as follows: 1 cycle 98 °C for 30 s; 15 cycles 98 °C for 10 s, 60 °C for 30 s, 72 °C for 30 s; 1 cycle 72 °C for 5 min; keep at 10 °C. After purification, the library was validated by Agilent 2100 Bioanalyzer. Qualified libraries were sequenced on the Illumina Sequencing Platform (HiSeq™ 2500) to produce 125 bp paired-end reads.

NGS QC Toolkit was used to evaluate and control the quality of raw data files obtained from the Illumina Sequencing Platform [17]. The reads containing poly-N and low-quality reads were removed to obtain clean reads, which were then mapped to the reference genome using HISAT2 [18]. The gene expression level was calculated with the fragments per kb per million reads (FPKM) method [19]. Differentially expressed genes (DEGs) were identified through the negative binomial distribution (NB) test, and the significance of the differences was estimated by the base mean value. On the basis of hypergeometric distribution, Gene Ontology (GO) enrichment and Kyoto Encyclopedia of Genes and Genomes (KEGG) pathway enrichment analysis of DEGs were performed using The R Programming Language [20].

2.4. Measurement of mantle edge pigmentation

The mantle edge pigmentation values (MPV) of the oysters was measured according to the method described by De Xing et al. [21] and Debecker et al. [22], with some modifications. The mantle edge (0.10 g) was dissected from each oyster and placed in a centrifugal tube containing 1 mL of 1.0 M NaOH. The samples were then incubated in a water bath at 80 °C for 2 h and centrifuged at 12 000 g for 10 min. Supernatants were transferred to a spectrophotometer to analyze the total melanin content at 400 nm absorbance (A400). The A400 values were used to represent the total melanin content, and the absorbance values of extracts in pathlength cuvettes were read to the last three decimal places.

2.5. Physiological assays

Each mantle sample (1:10, w:v) from the WSO or BSO group was homogenized in ice-cold lysis buffer (0.01 mM Tris, 0.0001 mM EDTA-2Na, 0.01 mM sucrose, 0.8% NaCl, pH 7.4), and then subjected to the activity assays. The TYR content (Mollusk Tyrosinase Elisa Kit) was determined by the tetramethylbenzidine method using a commercial kit (Nanjing Jiancheng Bioengineering Institute, China). The increase in the percentage of Caspase-3 activity was assayed by Caspase-3 Colorimetric Assay Kit (CASP3, BC3830, Solarbio Science & Technology

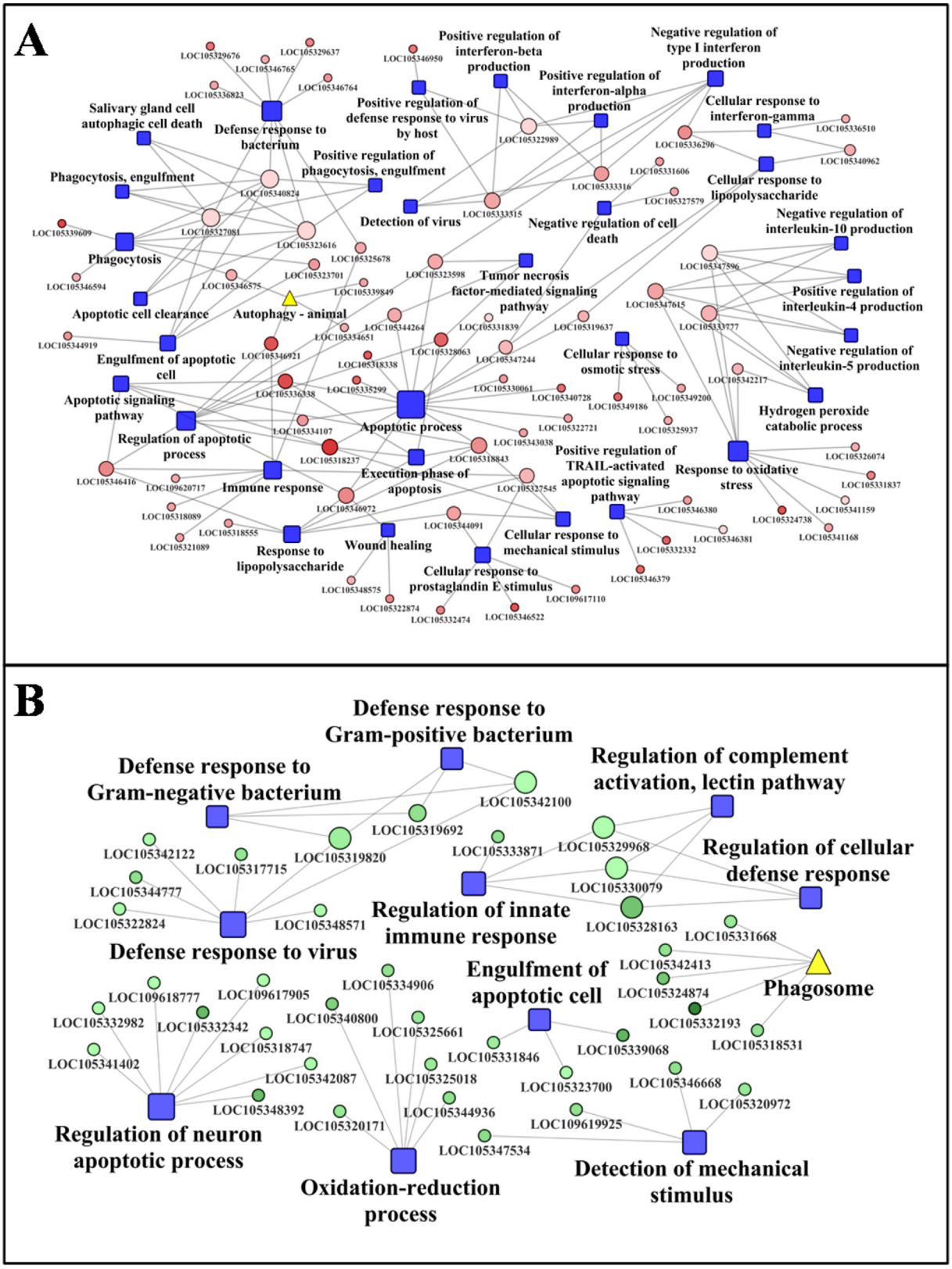

Fig. 5. Schematic illustration of different immunity strategies in black-shelled Pacific oysters (BSO) and white-shelled Pacific oysters (WSO), respectively, based on GO and KEGG enrichment analysis. (A) The immunity strategies in BSO. (B) The immunity strategies in WSO. Circles indicate differential expression genes (green ones represent down-regulated genes and red ones represent up-regulated genes); yellow triangle indicate the KEGG pathway; blue round rectangle indicate GO terms. (For interpretation of the references to color in this figure legend, the reader is referred to the Web version of this article.)

Co.,Ltd, China). Measurements of anti-superoxide anion radical (ASOR, A052), suppression of hydroxyl radical (•OH) (SHR, A018), total antioxidant capacity (T-AOC, A015) and peroxidase (POD, A084-1) were performed using commercial enzyme kits (Nanjing Jiancheng Bioengineering Institute, China). Taking bovine serum albumin as the standard, the protein concentration (A045-4) was determined by Bradford method [23].

2.6. Assessment of reactive oxygen species production using flow cytometry

The concentration of intracellular reactive oxygen species (ROS) was measured by fluorescent probe DCFH-DA. Fresh mantle tissues were crushed by eye scissors and separated into a single cell suspension by 0.25% trypsin at 37 °C. After being treated for 30 min, the mantle cells were collected and washed twice with cold PBS. The cells were then centrifuged at 500 × *g* for 10 min at 4 °C and the supernatant was discarded. 10^6 cells in each group were suspended in 500 μL of PBS and then incubated with 10 μM DCFH-DA at 37 °C for 30 min in the dark. The stained cells were immediately analyzed by flow cytometry (BD FACSCalibur™ Flow Cytometer, USA) with excitation and emission wave lengths of 488 and 530 nm, respectively. FlowJo Software 10.0 (USA) was used to analyze the data.

2.7. qRT-PCR

qRT-PCR was used to further confirm the gene expression level with 6 individuals in each group. Total RNA was treated with DNase I (Promega, USA) and the cDNA was then synthesized with Reverse Transcriptase M-MLV kit (Promega, USA) according to the manufacturer's instructions. The target genes were then assayed by SYBR Green on Bio-Rad CFX Connect™ Real-Time PCR Detection System, with ribosomal protein S18 (*RS18*) as an endogenous control [24]. All the primers used in this assay are listed in Table S1. The amplification efficiency of each primer pair was calculated by the dilution series of cDNA (1:10 for reference genes and 1:5 for genes of interest). PCR amplification was performed at 20 μL volume, with 10 μL SYBR Green PCR Master Mix, 2 μL diluted cDNA, 0.8 μL primers (5 μmol/L), and 7.2 μL DEPC-treated water. The thermal profile was 50 °C for 2 min, 94 °C for 10 min followed by 40 cycles of 9 °C for 5 s, 55 °C for 15 s, and 72 °C for 10 s. The relative expression levels of these genes were analyzed by the $2^{-\triangle\triangle CT}$ method [25,26].

2.8. Statistical analysis

One-way analysis of variance (one-way ANOVA) was used to analyze gene expression and physiology changes by SPSS 16.0 statistical software. $P < 0.05$ were considered statistically significant.

Principal component analysis (PCA) used GGEBiplot of The R Programming Language to evaluate the variability associated with physiological indicators (TYR, CASP3, ASOR, SHR, T-AOC, POD, and ROS).

3. Results and discussion

3.1. Fundamental physiological differences between BSO and WSO

The ODV and MPV results of BSO and WSO were shown in Fig. 1C. The average grayscale-based ODV of BSO and WSO were 0.98 and 0.32, respectively, indicating that BSO had more melanin pigmentation than WSO ($P < 0.01$). The average absorbance-based MPV of BSO and WSO were 1.79 and 1.26, respectively, indicating that the mantles of BSO also has greater melanin pigmentation than those of WSO ($P < 0.01$). Both results reinforce previous findings [1,15], which indicated that pigmentation in the shells of Pacific oyster was positively correlated with pigmentation in the mantles, suggesting that the darker the shell color is, the darker the mantle color is. In this study, the upregulation of TYR content and expression of 4 Tyr genes (LOC105344040, LOC105346503, LOC105348943, and LOC105320007) were accompanied by increased melanin pigmentation in BSO mantles ($P < 0.05$, Fig. 1C). The above results demonstrated the fundamental physiological differences between BSO and WSO.

3.2. Molecular differences between BSO and WSO mantles

Of the total reads (47 177 274 and 46 591 402), 70.06% and 70.42% were uniquely mapped to the oyster reference genome assembly in BSO and WSO, respectively (Table S2). A total of 1288 genes were identified as DEGs in mantles by comparing BSO and WSO ($P < 0.05$). The DEGs from BSO mantles had more genes upregulated compared with WSO mantles (735 genes versus 553 genes, respectively) (Table S3). The expression of randomly selected 5 DEGs was verified by qRT-PCR (Fig. S1).

GO enrichment analysis showed that, in the molecular function classification, most DEGs were enriched in metalloendopeptidase inhibitor activity and POD activity. Metallothionein can be used as an inhibitor for tyrosinase [27], and metalloendopeptidase inhibitor could regulate the activity of metallothionein, thereby regulating the expression of *Tyr* genes in BSO. PODs are kind of oxidoreductases, and these DEGs may be involved in the processes of response to oxidative stress. In the classification of cell components, DEGs (116/1288) are mainly concentrated in extracellular area and extracellular space. Based on KEGG enrichment, the pathways of 'extracellular matrix–receptor interaction' also showed significant differences, suggesting the secreting function of mantle tissues in Pacific oysters.

In order to further understand the classification of DEGs, only significant changes ($P < 0.05$) in GO biological process (BP) terms and KEGG pathways were considered as differential ones. Among them, 97 up-regulated and 48 down-regulated BP terms, and 6 up-regulated and 3 down-regulated KEGG pathways in BSO were compared with WSO.

The functional properties of these identified unigenes were classified by searching non-redundant (NR) database (ftp://ftp.ncbi.nih.gov/blast/db). Compared with WSO, the up-regulated BP terms in BSO could be classified in 8 categories, including the regulation of calcium ion and calcification, nerve conduction and signaling pathway, protein metabolism, energy and primary metabolism, tissue organization, immune function, stress responses and other cellular processes (Table S4). Compared with BSO, the up-regulated BP terms in WSO involved cytoskeleton structure, nerve conduction and signaling pathway, protein metabolism, morphogenesis and development, immune function and other cellular processes (Table S5).

The hierarchy and network of GO BP items were classified and integrated by using BinGO enrichment analysis method, and BP items with family-wise error rate (FWER) < 0.05 were further screened. Fig. 2 summarized that responses to stimulus, biological regulation, muti-organism process, death and immune system process, etc were significantly up-regulated in BSO. Fig. 3 summarized that multicellular organismal process, developmental process, multicellular organismal development, cell development and spermatid development were significantly up-regulated in WSO.

The up-regulated KEGG pathways in BSO were ABC transporters, tyrosine metabolism, aminoacyl-tRNA biosynthesis, ubiquitin mediated proteolysis, fatty acid metabolism and autophagy-animal. And the up-regulated KEGG pathways in WSO were ECM-receptor interaction, phagosome and purine metabolism (Table S6).

Based on the above results, BSO and WSO may have different characteristics in the molecular modulation mechanism, respectively.

3.3. Some physiological evidences for molecular differences

To verify the physiological differences between BSO and WSO, TYR, CASP3, ASOR, SHR, ROS, T-AOC and POD were detected and compared by PCA analysis (Table S7). Two main factors were extracted from the

PCA results to explain 51.20% of the total data variance. The first component (PC1) accounted for 31.41% of the total variance. The results showed that the WSO sits on the positive side of the PC1 axis, while the most BSO sits on the negative side of the PC1 axis. (Fig. 4). High levels of TYR, CASP3 and SHR and low levels of ROS in BSO defined this separation. The second component (PC2) explained 19.79% of the total variance, with BSO and WSO falling almost on the same side of PC2.

In this study, BSO showed a significant increase in TYR content and CASP3 activity compared with WSO, suggesting that the processes of melanin synthesis and apoptosis were up-regulated in BSO. However, in the mantles of BSO versus WSO, there was no difference in the levels of the antioxidant POD and T-AOC. These might demonstrate the enrichment analysis that BSO and WSO both could response to oxidative stress though they maybe use different strategy. However, different ROS contents and free radical scavenging capacity may indicate different antioxidant patterns between BSO and WSO. ROS are a major form of free radicals, with superoxide anion (O_2·-) and hydroxyl (•OH) free radicals being the important components [28–30]. Previous studies have shown that the rapid elimination of excess free radicals is vital in maintaining normal cell metabolism and improving the body's resistance and immunity [31]. Pacific oyster with the high level of melanin content, may also have the high performance of scavenging free radicals.

3.4. Immune recognition and modulation

The up-regulated BP terms in BSO (Table S4) suggested that there might be some difference between BSO and WSO in response to immune antigens. Although both BSO and WSO showed defensive responses to bacteria and viruses (Table S4, S5), DEGs related to response to lipopolysaccharide, interferon, and prostaglandin, were up-regulated in BSO, suggesting that the BSO may be more sensitive to immune substances. Negative or positive regulations of interleukins and interferons were up-regulated in BSO, and the regulation of complement activation and lectin pathway was up-regulated in WSO, indicating that there may exist different immune modulations between BSO and WSO.

3.5. Apoptosis and phagocytosis

Enrichment analysis also showed that the apoptotic process and phagocytosis of BSO and WSO may be carried out in different ways. There were more up-regulated DEGs of the apoptotic process in BSO than WSO (24 versus 11), including the caspase-3 gene (*Casp3*, LOC105318843, LOC105346972), which could promote cell apoptosis [32]. Increased activity of caspase-3 protein was also detected (Table S7). The 5 up-regulated tumor necrosis factors (*Tnf* related genes, including LOC105319637, LOC105323598, LOC105344264, LOC105346921, LOC105344264) in BSO, suggesting that TNF family may play a vital role in activating cell apoptosis and phagocytosis in BSO. The KEGG pathway 'autophagy-animal' was up-regulated in BSO, but 'phagosome' was up-regulated in WSO, which suggested the phagocytosis in WSO is more dependent on phagocyte-like macrophage (LOC105324874). On the contrary, the cellular substances, such as cathepsin L (LOC105334651) and halomucin (LOC105339849) may play an autophagic role in BSO.

3.6. Oxidative stress

RNA-Seq analysis (Table S3) showed that there were 7 types of up-regulated *Pods* (LOC105324738, LOC105331837, LOC105341159, LOC105341168, LOC105342217, LOC105347596, LOC105347615) in BSO, which resulted in a significant up-regulation of the 'response to oxidative stress' in biological processes in BSO, and an up-regulation of the 'oxidation-reduction process' in biological processes in WSO, because of the up-regulated retinal dehydrogenase (*Rdh*, LOC105334906) and flavin-containing monooxygenase (LOC105325018, LOC105340800). Antioxidant enzymes control the toxic effects of ROS produced in different cellular compartments. Peroxisomes, which are important cell organelles involved in oxidative metabolism, contain PODs, thus contributing to the cellular production of ROS [33]. Therefore, the production of PODs maybe an important pathway of response to oxidative stress in BSO. So, different oxidation-related pathways were enriched in both BSO and WSO, suggesting the different response strategies of BSO and WSO to oxidative stress.

4. Conclusions

This study investigated the molecular and physiological differences between BSO and WSO. Different immunity-related BP terms and KEGG pathways between BSO and WSO were visualized in Cytoscape 3.4.0 (Fig. 5).

The results showed that there may be some differences between BSO and WSO in immune recognition and modulation, as well as in the mode of apoptosis and phagocytosis, and the different response strategies to oxidative stress.

Acknowledgments

This research was supported by National Key R&D Program of China (No. 2018YFD0901400), The National Natural Science Foundation of China (No. 41876193), The Key R & D Program of Shandong Province, China (No. 2018GHY115027), Special Funds for Taishan Scholars Project of Shandong Province, China (No. tsqn201812094), The Shandong Provincial Natural Science Foundation, China (Nos. ZR2019MC002 and ZR2017BC058), A Project of Shandong Province Higher Educational Science and Technology Program (No. J17KA129), The Modern Agricultural Industry Technology System of Shandong Province, China (No. SDAIT-14-03), and The Key R&D Program of Yantai City, China (No. 2017ZH054).

Appendix A. Supplementary data

Supplementary data to this article can be found online at https://doi.org/10.1016/j.fsi.2019.05.056.

References

[1] K. Jung-Ha, K. Hyun-Sook, L. Jung-Mee, A. Chel-Min, K. Sung-Youn, L. Yun-Mi, K. Jong-Joo, Characterizations of shell and mantle edge pigmentation of a pacific oyster, *Crassostrea gigas*, in Korean peninsula, Asian-australasian Journal of Animal Sciences 26 (12) (2013) 1659–1664.
[2] S. Hao, X. Hou, L. Wei, J. Li, Z. Li, X. Wang, Extraction and identification of the pigment in the adductor muscle scar of pacific oyster *Crassostrea gigas*, PLoS One 10 (11) (2015) e0142439.
[3] S.T. Williams, S. Ito, K. Wakamatsu, T. Goral, N.P. Edwards, R.A. Wogelius, T. Henkel, L.F. de Oliveira, L.F. Maia, S. Strekopytov, Identification of shell colour pigments in marine snails *Clanculus pharaonius* and *C. margaritarius* (trochoidea; gastropoda), PLoS One 11 (7) (2016) e0156664.
[4] S. Savitha, W. Sushama, G. Raman, Melanosomal proteins–role in melanin polymerization, Pigm. Cell Res. 15 (2) (2010) 127–133.
[5] J.Y. Lin, D.E. Fisher, Melanocyte biology and skin pigmentation, Nature 445 (7130) (2007) 843–850.
[6] L. Jacquin, P. Lenouvel, C. Haussy, S. Ducatez, J. Gasparini, Melanin-based coloration is related to parasite intensity and cellular immune response in an urban free living bird: the feral pigeon Columba livia, J. Avian Biol. 42 (1) (2011) 11–15.
[7] S. Manickam, Comparative biochemistry of eumelanogenesis and the protective roles of phenoloxidase and melanin in insects, Pigm. Cell Res. 15 (1) (2010) 2–9.
[8] N.D. Pugh, B. Premalatha, L. Hemant, F.E. Dayan, J. Vaishali, B. Erdal, M. Toshiaki, M. Rita, K. Ikhlas, D.S. Pasco, Melanin: dietary mucosal immune modulator from *Echinacea* and other botanical supplements, Int. Immunopharmacol. 5 (4) (2005) 637–647.
[9] D.S. Alviano, A.J. Franzen, L.R. Travassos, H. Carla, R. Sonia, E. Regina, C.S. Alviano, M.L. Rodrigues, Melanin from *Fonsecaea pedrosoi* induces production of human antifungal antibodies and enhances the antimicrobial efficacy of phagocytes, Infect. Immun. 72 (1) (2004) 229–237.
[10] M.H.T. Stappers, A.E. Clark, V. Aimanianda, S. Bidula, D.M. Reid, P. Asamaphan, S.E. Hardison, I.M. Dambuza, I. Valsecchi, B. Kerscher, A. Plato, C.A. Wallace, R. Yuecel, B. Hebecker, M. da Glória Teixeira Sousa, C. Cunha, Y. Liu, T. Feizi,

A.A. Brakhage, K.J. Kwon-Chung, N.A.R. Gow, M. Zanda, M. Piras, C. Zanato, M. Jaeger, M.G. Netea, F.L. van de Veerdonk, J.F. Lacerda, A. Campos, A. Carvalho, J.A. Willment, J.-P. Latgé, G.D. Brown, Recognition of DHN-melanin by a C-type lectin receptor is required for immunity to *Aspergillus*, Nature 555 (2018) 382.

[11] K. Y-J, H. Uyama, Tyrosinase inhibitors from natural and synthetic sources: structure, inhibition mechanism and perspective for the future, Cell. Mol. Life Sci. 62 (15) (2005) 1707–1723.

[12] R. Takgi, T. Miyashita, A cDNA cloning of a novel alpha-class tyrosinase of *Pinctada fucata*: its expression analysis and characterization of the expressed protein, Enzym. Res. (2014) 1–9.

[13] Z. Guofan, F. Xiaodong, G. Ximing, L. Li, L. Ruibang, X. Fei, Y. Pengcheng, Z. Linlin, W. Xiaotong, Q. Haigang, The oyster genome reveals stress adaptation and complexity of shell formation, Nature 490 (7418) (2012) 49–54.

[14] Y. Xue, Y. Hong, K. Lingfeng, G. Fengguang, Z. Guan, L. Qi, Molecular cloning and differential expression in tissues of a tyrosinase gene in the Pacific oyster *Crassostrea gigas*, Mol. Biol. Rep. 41 (8) (2014) 5403–5411.

[15] W. Yu, C. He, Z. Cai, F. Xu, L. Wei, J. Chen, Q. Jiang, N. Wei, Z. Li, W. Guo, A preliminary study on the pattern, the physiological bases and the molecular mechanism of the adductor muscle scar pigmentation in pacific oyster *Crassostrea gigas*, Front. Physiol. 8 (2017) 699.

[16] J. Brake, F. Evans, C. Langdon, Evidence for genetic control of pigmentation of shell and mantle edge in selected families of Pacific oysters, *Crassostrea gigas*, Aquaculture 229 (1) (2004) 89–98.

[17] R.K. Patel, J. Mukesh, NGS QC Toolkit: a toolkit for quality control of next generation sequencing data, PLoS One 7 (2) (2012) e30619.

[18] K. Daehwan, L. Ben, S.L. Salzberg, HISAT: a fast spliced aligner with low memory requirements, Nat. Methods 12 (4) (2015) 357–360.

[19] T. Cole, B.A. Williams, P. Geo, M. Ali, K. Gordon, M.J. Baren, Van, S.L. Salzberg, B.J. Wold, P. Lior, Transcript assembly and quantification by RNA-Seq reveals unannotated transcripts and isoform switching during cell differentiation, Nat. Biotechnol. 28 (5) (2010) 511–515.

[20] K. Minoru, A. Michihiro, G. Susumu, H. Masahiro, H. Mika, I. Masumi, K. Toshiaki, K. Shuichi, O. Shujiro, T. Toshiaki, KEGG for linking genomes to life and the environment, Nucleic Acids Res. 36 (2008) 480–484.

[21] D. Xing, L. Qi, L. Kong, Y. Hong, D. Xing, L. Qi, L. Kong, Y. Hong, Heritability estimate for mantle edge pigmentation and correlation with shell pigmentation in the white-shell strain of Pacific oyster, *Crassostrea gigas*, Aquaculture 482 (2018) 73–77.

[22] S. Debecker, R. Sommaruga, T. Maes, R. Stoks, Larval UV exposure impairs adult immune function through a trade-off with larval investment in cuticular melanin, Funct. Ecol. 29 (10) (2015) 1292–1299.

[23] M.M. Bradford, A rapid and sensitive method for the quantitation of microgram quantities of protein utilizing the principle of protein-dye binding, Anal. Biochem. 72 (1) (1976) 248–254.

[24] H. Miyamoto, K. Kajihara, Conserved ribosomal protein sequences S5, S18, S27, S30 in the pacific oyster Crassostrea gigas and Crassostrea virginica, Mem. School of Biol.-Orient. Sci. Technol. Kinki Univ. 16 (2005) 1–5.

[25] K.J. Livak, T.D. Schmittgen, Analysis of relative gene expression data using real-time quantitative PCR and the $2^{-\Delta\Delta CT}$ Method, Methods 25 (4) (2001) 402–408.

[26] S.A. Bustin, V. Benes, J.A. Garson, J. Hellemans, J. Huggett, M. Kubista, R. Mueller, T. Nolan, M.W. Pfaffl, G.L. Shipley, J. Vandesompele, C.T. Wittwer, The MIQE guidelines: minimum information for publication of quantitative real-time PCR experiments, Clin. Chem. 55 (4) (2009) 611–622.

[27] I. Bremner, Nutritional and physiologic significance of metallothionein, Methods Enzymol. 205 (1) (1991) 25–35.

[28] D. Ludovic, K. Edouard, L.G.C. Nelly, L. Christophe, A.K. Volety, S. Philippe, Reactive oxygen species in unstimulated hemocytes of the pacific oyster *Crassostrea gigas*: a mitochondrial involvement, PLoS One 7 (10) (2012) e46594.

[29] R.S. Anderson, *Perkinsus marinus*secretory products modulate superoxide anion production by oyster (*Crassostrea virginica*) haemocytes, Fish Shellfish Immunol. 9 (1) (1999) 51–60.

[30] R.S. Anderson, K.T. Paynter, E.M. Burreson, Increased reactive oxygen intermediate production by hemocytes withdrawn from *Crassostrea virginica* infected with *Perkinsus marinus*, Biol. Bull. 183 (3) (1992) 476–481.

[31] N.K. Vate, S. Benjakul, Antioxidative activity of melanin-free ink from splendid squid (*Loligo formosana*), Int. Aquat. Res. 5 (1) (2013) 1–12.

[32] A.G. Porter, R.U. Janicke, Emerging roles of caspase-3 in apoptosis, Cell Death Differ. 6 (2) (1999) 99–104.

[33] L.A.D. Río, F.J. Corpas, L.M. Sandalio, J.M. Palma, M. Gómez, J.B. Barroso, Reactive oxygen species, antioxidant systems and nitric oxide in peroxisomes, J. Exp. Bot. 53 (372) (2002) 1255–1272.